Biochemistry and Biophysics Reports 6 (2016) 203–208

Contents lists available at ScienceDirect

Biochemistry and Biophysics Reports

journal homepage: www.elsevier.com/locate/bbrep

Dynamic response of HPV16/anti-HPV16 pairs with unbinding events studied by atomic force microscopy

Shiming Lin [a,*,1], Chung-Hung Hong [a,b,1], Bor-Ching Sheu [a], Long-Xin Wu [a], Wan-Chen Huang [a], Wei-Chih Huang [a], Cheng-Yan Guo [a]

[a] Institute of Medical Device and Imaging, National Taiwan University, Taipei, Taiwan
[b] Graduate Institute of Electronics Engineering, National Taiwan University, Taipei, Taiwan

ARTICLE INFO

Article history:
Received 9 January 2016
Received in revised form
11 April 2016
Accepted 14 April 2016
Available online 16 April 2016

Keywords:
Atomic force microscopy
HPV16
Anti-HPV16 L1
Unbinding force

ABSTRACT

This paper proposes an effective approach to distinguish whether samples include Human Papilloma virus type-16 (HPV16) by Atomic force microscopy (AFM). AFM is an important instrument in nano-biotechnology field. At first we identified the HPV16 by Polymerase chain reaction (PCR) analysis and Western blotting from specimen of the HPV patient (E12) and the normal (C2), and then we used an AFM to observe the surface ultrastructure by tapping mode and to measure the unbinding force between HPV16 coupled to an AFM tip and anti-HPV16 L1 coated on the substrate surface by contact mode. The experimental results by tapping mode show that the size of a single HPV viron was similar to its SEM image from the previous literatures; moreover, based on the purposed methods and the analysis, two obvious findings that we can determine whether or not the subject is a HPV patient can be derived from the results; one is based on the distribution of unbinding forces, and the other is based on the distribution of the stiffness. Furthermore, the proposed method could be a useful technique for further investigating the potential role among subtypes of HPVs in the oncogenesis of human cervical cancer.

1. Introduction

Recent years have seen increased attention being given to Human papilloma virus (HPV) in biomedicine field literature. Because a number of studies have shown that HPV infection is an important risk factor for cervical cancer [1–3], breast cancer [4–6], and even lung cancer [7]. Especially the relation between suffering from cervical cancer and HPV16/18 has massive empirical support in clinical observation respect [1,8]. Besides, HPV is one kind deoxyribonucleic acid (DNA) virus. In general, HPV itself vanishes after infecting the cervix about 7–8 months, but a small part still survives and proceeds to make the cervix be infected with this type pathogen. HPV is so a type of very tiny pathogen (nanometer level) that finding a suitable observational instrument is a very important task. Traditionally, methods for detecting HPV in cervical samples include Southern blot and dot blot hybridization [9], Hybrid Capture II (HCII) [10], etc. In addition to the above-described methods, the way to detect HPV by atomic force microscope (AFM) is perhaps more efficient, simple and convenient.

AFM, invented by Binning, Calvin Quate, and Gerber in 1986 as a tool with high-resolution, now has many applications in the fields of molecular biology, semiconductor physics, etc [11–13]. Because AFM has so many applications, in the past 30 years the science and technology for the creation and use of AFM has progressed tremendously. In the field of molecular biology, AFM has proved to be applicable to structural studies of single biomolecules [14–16] and to the measurement of molecular forces at the single-molecule level by contact mode. AFM has the absolute predominance of nano-level spatial resolution for detecting molecular interaction at high lateral resolution combined with immense force sensitivity in an intricately physiologic environment as compared with other biophysical approaches to direct measurements of inter-molecular forces, such as the magnetic torsion, the bio-membrane force probe (BFP), etc. Therefore, AFM has been utilized well to gauge and estimate inter-molecular forces between various ligand and receptor pairs [17–19] and intra-molecular unfolding forces of individual proteins [20].

AFM is perhaps the most versatile member among microscopes known as scanning probe microscopes (SPMs). For example, to achieve specific needs, we can change the characteristics of AFM tips, such as chemical modification [21], and different chemical modification of AFM tips may have different properties. Thus we can acquire the information about specific force between modified tips and local area of samples by contact mode. For measurements of intermolecular binding strengths between antibody and antigen

* Correspondence to: Institute of Medical Device and Imaging, National Taiwan University/College of Medicine, No.1, Sec.1, Jen-Ai Road, Taipei, Taiwan.
E-mail address: til@ntu.edu.tw (S. Lin).
[1] These authors contributed equally to this work.

http://dx.doi.org/10.1016/j.bbrep.2016.04.008

binding, antibodies are attached to AFM tips and antigens are attached to substrate surfaces, and vice versa. The modified AFM tip is brought into contact with the substrate surface so as to form antibody/antigen complexes. When the modified AFM tip is retracted from the substrate surface, the force required for dissociation (unbinding force), defined as the rupture force at the moment of sample separation, can subsequently be measured and recorded by pulling on the complexes until the interaction bond breaks. Some studies provide methods for estimation of affinity, rate constants, and bond width of the binding pocket [22–24], and even provide a tool for mapping the energy landscape [25]. In addition, these equipments provide insights into the molecular dynamics of the receptor/ligand recognition process by varying the loading rate of force application [22–25]. In this study, we propose a method for the biosensor application of AFM to studies of the molecular dynamics of the HPV16/anti-HPV16 recognition process based on clinical cantilever mechanical theories.

2. Material and methods

2.1. Polymerase chain reaction (PCR)

PCR is one kind technique in the molecular biology field, and it lets a specific DNA sequence to be copied. Such technique was performed as previously described [26]. This study used PCR technique to copy and produce a large number specific HPV16 E6 primer segments from the HPV16 patient, and then by the same method to produce a large amount of HPV16 E6 gene segments. Next we confirmed whether the specimen includes HPV16 by comparing to above-mentioned two kinds segments electrophoresis patterns.

2.2. Western blot analysis

Western blot analysis is widely used method to confirm specific proteins in a sample, and the detailed analysis procedure was performed as previously described [27]. This study used western blot analysis and the results of electrophoresis to confirm whether HPV16 existed in the specimen.

2.3. AFM contact mode and tapping mode

AFM contact mode is often used to measure the force interaction between the AFM tips and samples [22–25]. But AFM contact mode is easy to destroy the surface appearances of samples. To overcome the problem, we can use AFM tapping mode as a solution to obtain original AFM images [28].

2.4. AFM images of HPV16 acquired by tapping mode

The images of HPV16 were obtained by using an Atomic force microscopy (SPA 300HV, Seiko Instruments Inc., Japan). Commercial silicon cantilevers (SuperSharpSilicon™ SSS-SEIH, NANOSENSORS, Switzerland) were used in tapping mode in air, and then topographic images were acquired by using a resonant frequency of 140 kHz for the probe oscillation.

2.5. Functionalization of AFM tips and the substrate surface

The mica substrate surface coated with HPV16 from the specimen that had checked by PCR and western blot analysis and AFM tips (PointProbePlus, Nanosensors, Switzerland) were coupled with anti-HPV16 L1, and moreover, the functionalization procedure is described as follows. AFM tips and the substrates were immersed in 65% solution of nitric acid for 10 min and then were taken out. These AFM tips and the substrates were then immersed in 5% ethanol solution for 10 min at room temperature, followed by several rinses with solution of 5% ethanol/95% distilled water, and then these AFM tips and the substrates were immersed in 5% 3-APTES solution in phosphate-buffered saline (PBS, pH 7.2) for 45 min and then extensively rinsed with PBS solution. Next, these AFM tips and the substrates were immersed in a 2.5% Glutaraldehyde solution for 75 min In the last step, the anti-HPV16 L1 solution (200 μg/ml in PBS, pH 7.2) bound covalently to the AFM tips for overnight incubation at 4 °C. On the other hand, before AFM force measurements, the mica substrates were covalently bond with HPV16 sample (E12) solution in PBS (pH 7.2) for 2 h.

2.6. AFM force measurement acquired by contact mode

A scanning probe microscope (SPM) system measuring head (SMENA liquid head, NTMDT, Moscow, Russia) was used to measure the interaction force between HPV16 and anti-HPV16 L1 in liquid environment. All AFM force measurements were executed at the same loading rate 333.3 nm/s in PBS buffer (pH 7.2). Besides, the interaction force between HPV16 and anti-HPV16 probe was measured by approaching the AFM tip towards the HPV16 sample perpendicularly.

3. Results and discussion

3.1. AFM images of HPV16

The detailed surface topographies of HPV16 samples on the substrate were observed by use of AFM tapping mode (Fig. 1); moreover, Fig. 1A-F shows the AFM images of the HPV particles on the mica substrate. Fig. 1A shows the AFM image (scanning area 2000 nm × 2000 nm) of the HPV samples, and the HPV particles appear to be mainly spherical and uniformly distributed on the mica substrate. By zooming into the square area which displayed in Fig. 1A and B respectively, this higher resolution images (Fig. 1B and C) were obtained. This higher resolution images (Fig. 1 B and C) clearly display many separate spherical viral particles which exist on the surface. Besides, Fig. 1A', B', and C' are three-dimensional images of Fig. 1A, B, and C, respectively. To research the dimension of a single in Fig. 1C, three viral particles which were marked by squares in Fig. 1C were zoomed in Fig. 1D-F (topographic images). More than 50 single HPV16 particles were then examined and analyzed by AFM imaging software, and their average diameter from the AFM images was 51.6 ±1.8 nm (mean ±SD, n=51), in agreement with the size estimated from electron microscopy apparently [29].

3.2. AFM force measurements acquired by contact mode and analysis

3.2.1. The specificity of HPV16/anti-HPV16

To understand the dynamic response relation between HPV16 and anti-HPV16 L1, we used AFM contact mode to measure the unbinding force required to separate complementary HPV16/anti-HPV16 L1 pairs. Besides, all AFM force measurements were implemented at the same loading rate of 333.3 nm per second in PBS buffer (pH 7.2). The interaction force between HPV16 and anti-HPV16 L1 probe was measured by approaching the tip towards the sample perpendicularly. Before executing the force vs. distance measurements of the antigen-antibody interaction, we must design and carry out experiments of control group and experimental group of unbinding events. The detailed all kinds of unbinding events results are described as follows.

Fig. 2A-C show typical examples of the force-distance curves

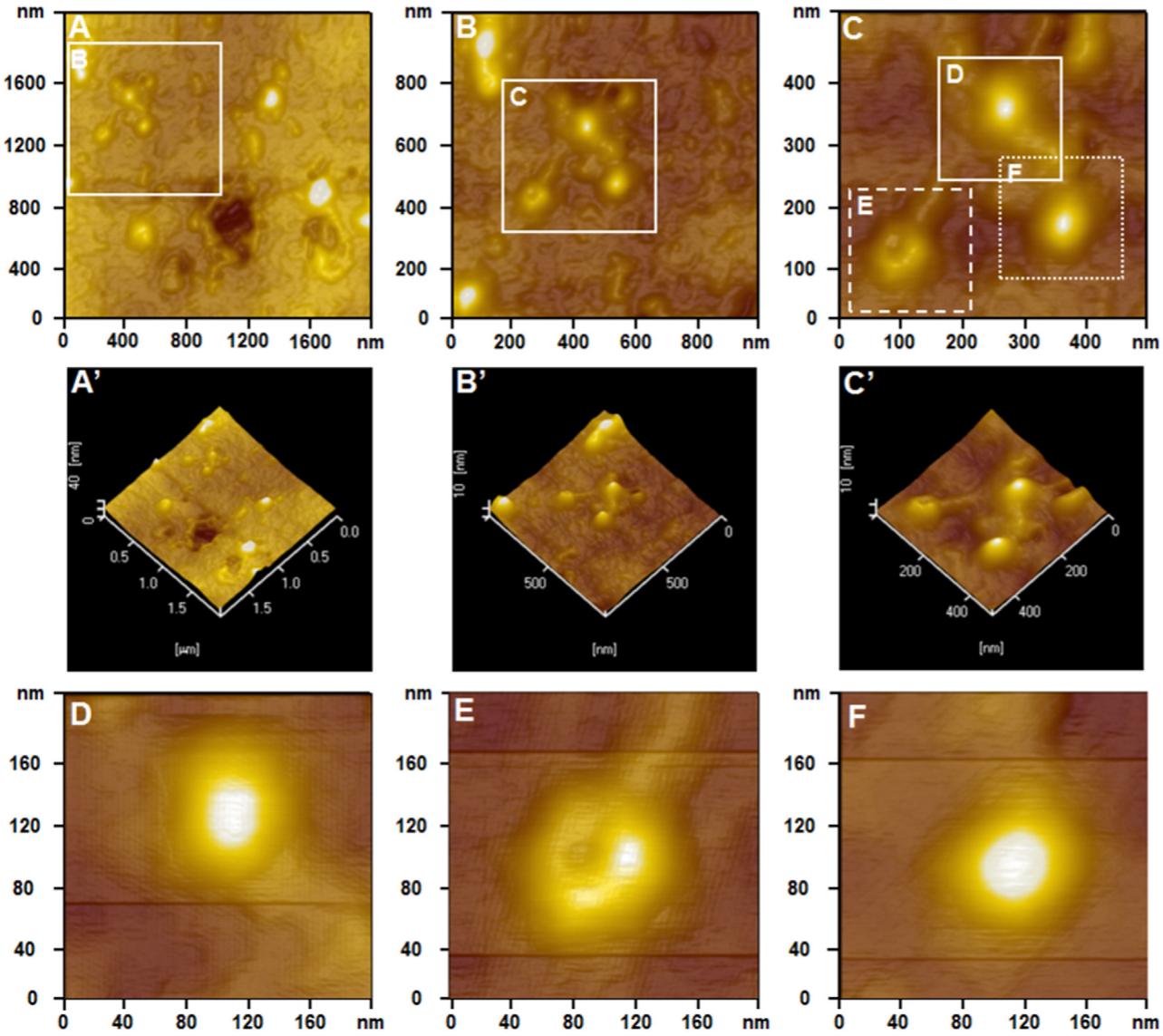

Fig. 1. AFM topographic images of the HPV on mica substrate acquired by tapping mode. (A) A two-dimensional topographic images (scanning area: 2000 nm × 2000 nm); (B) (scanning area: 1000 nm × 1000 nm) and (C) (scanning area: 500 nm × 500 nm) are two-dimensional topographic images which obtained by zooming into the square area in (A) and (B) respectively; (A'- C') are three-dimensional images of (A), (B) and (C) respectively; (D-F) are two-dimensional images (scanning area: 200 nm × 200 nm) which acquired by zooming into the three squares in (C).

obtained with these systems. In Fig. 2A, we acquire the result that no obvious pull-off event was observed in the tip-glass system. In the HPV16-anti-HPV16 L1 system (see Fig. 2B), an apparent force discontinuity was present as a result of the adhesion force between the HPV16-anti-HPV16 L1 pair. This reveals that the force measured in the HPV16-anti-HPV16 L1 system can belong to the specific HPV16-anti-HPV16 L1 unbinding event. Besides, in order to verify that HPV16-anti-HPV16 L1 binding brought about the observed the phenomenon of force discontinuity, the substrate was coating with proteins from the normal instead of HPV16 as a control experiment. We can find that the recorded force curves displayed no adhesion pull-off event (see Fig. 2C), that is to say, an unbinding force phenomenon was not observed. The two control experiments (see Fig. 2A and C) show that the lack of discrete adhesion points in the force-distance curves. In other words, these two control experiments highlights the specificity of the interaction between the anti-HPV16 L1 coupled to the AFM tip and the HPV16 coated to the substrate (as shown in Fig. 2B).

3.2.2. The HPV16 L1-anti-HPV16 L1 with mono-, di-, and multi-unbinding events

A series experimental and control experiments (as shown in Fig. 2A-C) show that the specific interaction forces between HPV16 and anti-HPV16 L1 exist. Besides, this paper reveals that the force curves with specific single, double, and multiple unbinding events were observed in this study. Fig. 3 shows the force-distance of the HPV16-anti-HPV16 L1 system with mono-(as shown in Fig. 3A), di-(as shown in Fig. 3B), and multi-(as shown in Fig. 3C) unbinding events recorded for a pH 7.2 solution, which may be attributed to a single, sequential, and multiple breaking of interacting bond (s) between HPV16 and anti-HPV16 L1 respectively. Schematic diagrams of the A, B, and C binding events are shown in a, b, and c, respectively. Besides, the force curve with one adhesion point (as shown in Fig. 3A) reveals that the single pair interaction was broken during the retraction process of the force measurement. This force curve (Fig. 3A) could be ascribed to the real situation that the HPV16 particle randomly immobilized on the substrate could be oriented (a1) or lying on the substrate (a2) with one

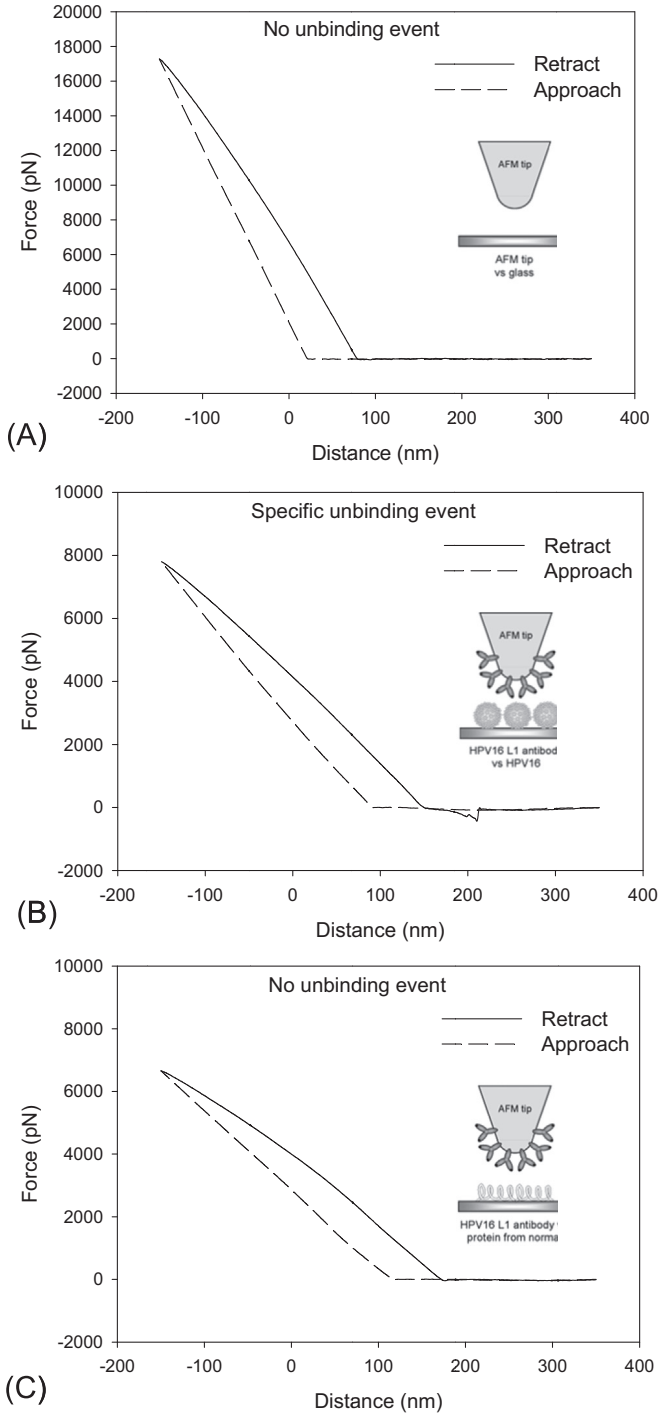

Fig. 2. Typical measurements of unbinding forces acquired by AFM contact mode. Force-distance curves of no adhesive force appeared during the retraction process, which were acquired by use of (A) AFM tip/glass and (C) HPV16 L1 antibody/protein from normal systems as two control experiments. (B) A representative force-distance curve of the HPV16-anti- HPV16 L1 system with a specific unbinding event which appeared during the retracting process.

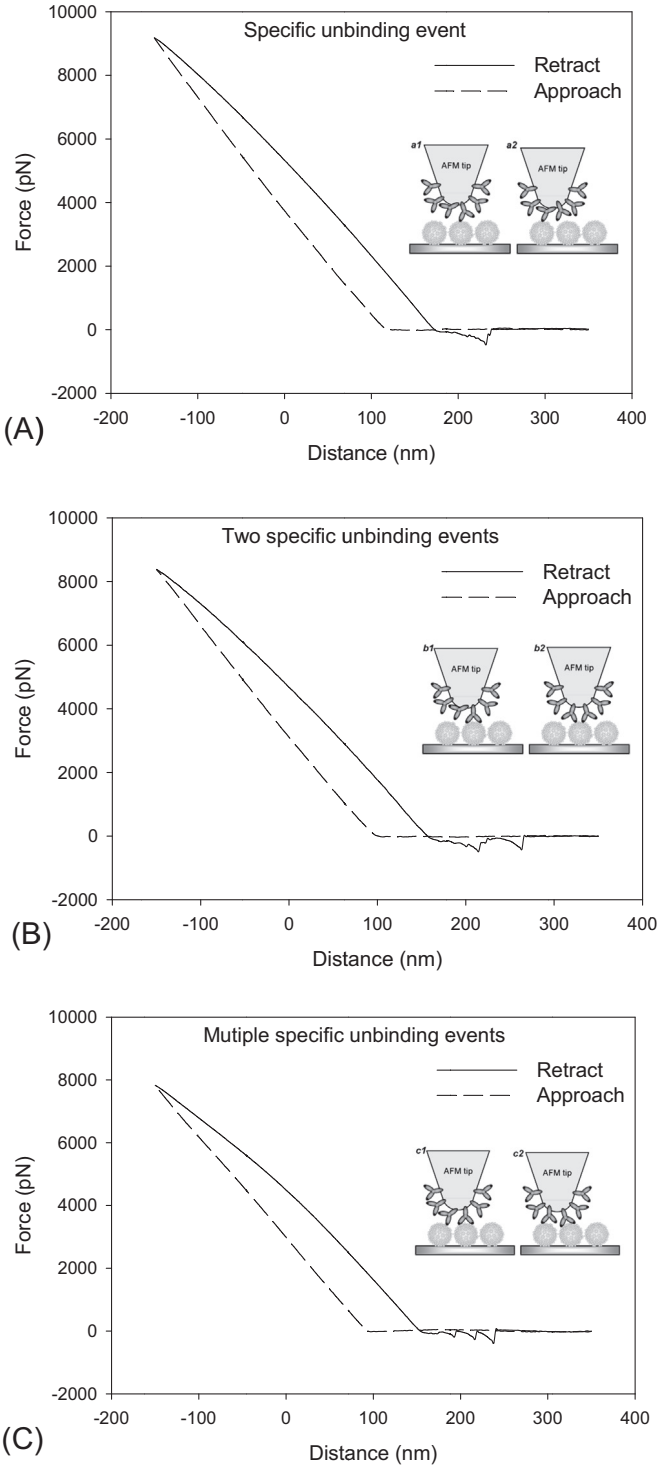

Fig. 3. Force-distance curves of the HPV16-anti-HPV16 L1 system with (A) mono-, (B) di, and (C) multi-unbinding events, which may be attributed to (A) a single, (B) sequential, and (C) multiple breaking of bond(s) between the substrate and the AFM tip. Schematic representations of the A, B, and C binding events are shown in *a*, *b*, and *c*, respectively. The HPV16 particles randomly immobilized on the substrate could be oriented (*a1*) or lying on the substrate (*a2*) with one binding site oriented to bind a single anti-HPV16 L1 on the AFM tip. Two separate anti-HPV16 L1 on the AFM tip can bind to two identical combining sites on one HPV16 (*b1*) or to separate combining sites on two HPV16 particles (*b2*). Several separate anti-HPV16 L1 molecules on the AFM tip can bind to three (*c1*) separate combining sites on HPV16 particles.

binding site oriented in order to bind a single anti-HPV16 on the AFM tip. Next, the force curve with two adhesion points (as shown in Fig. 3B) shows a sequential breaking of interacting bond(s) from the complementary HPV16/anti-HPV16 L1 pairs. In Fig. 3B, we can find that the HPV16 particle on the substrate might bind to two identical binding sites on one anti-HPV16 L1 (b1), or bind to separate binding sites on two anti-HPV16 L1 (b2). Besides, there were multiple pull-off steps during the retraction process in some force curves that could be ascribed to multiple breaking of interacting bonds between the anti-HPV16 L1 molecules on the AFM tip and the HPV16 particles on the substrate (see c1 and c2 in Fig. 3C).

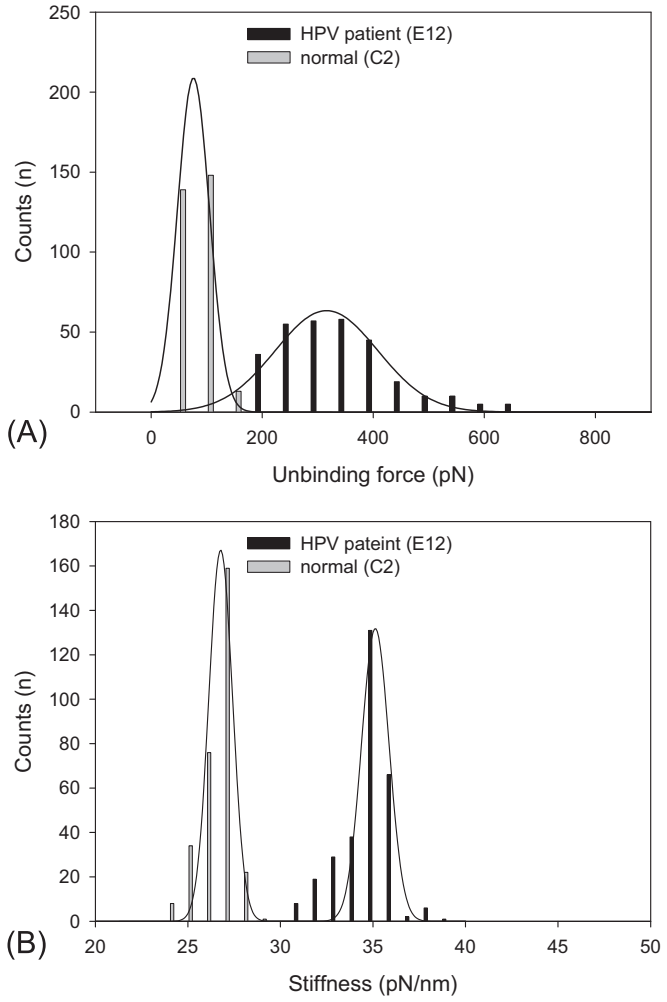

Fig. 4. Histograms and Gaussian distribution curves show differences in the (A) unbinding forces and (B) stiffness of the HPV patient (E12) and the normal (C2); counts were 300 and 300, respectively, performed at the same loading rate of 333.3 nm per second in PBS (pH 7.2).

3.3. Experimental results and the statistical analysis

To summarize the salient features of the experimental statistical analysis, two findings of the obviously statistical difference between the HPV patient and the normal are worthy of attention; one is the unbinding force (as shown in Fig. 4A), and the other is the stiffness (as shown in Fig. 4B). Fig. 4A shows the histograms of the unbinding force distribution between the HPV16 L1 and the anti-HPV16 L1 of the HPV patient and the normal, and the unbinding force was calculated from 600 force-distance curves; the amount of the HPV patient is 300, and the other is also 300. Fig. 4A shows the results of unbinding forces (mean ± SD) of the HPV patient samples (312.7 ± 99.9 nN) and of the normal samples (53.7 ± 24.6 nN), respectively. These data were examined by using one-way ANOVA, and the statistical analyses show significant differences among measurements in the two groups ($p < 0.05$). These results reveal that the unbinding forces for these two groups were strikingly different. Besides, these data were reasonable because the specificity relation between the HPV16 L1 and the anti-HPV16 L1, so the unbinding forces of the HPV patient samples are usually larger than the unbinding forces of the normal samples. Next, Fig. 4B shows that the stiffness distributions of the HPV patient (34.2 ± 1.3 pN/nm) and the normal (26.1 ± 0.9 pN/nm) are completely separate, and the statistical analyses still reveal significant difference among measurements in these two groups ($p < 0.05$), and the stiffness of the HPV patient is obviously larger than the stiffness of the normal. Such results (as shown in Fig. 4B) are reasonable because the shell of the HPV16 L1 consists of capsomeres and these capsomeres form a symmetrical icosahedral granule, and moreover, the shell structure of the HPV16 L1 (E12) is more stable and harder than the samples from the normal (C2) only include proteins.

4. Conclusions

This paper shows the advantage of using AFM, which is a sensitive force probe instrument and provides the high-resolution imaging of the HPV16 by AFM tapping mode to avoid destroying the samples surfaces. Besides, this paper proposes a label-free way to check whether or not the HPV16 molecules exist from the force specificity relation between HPV16 and anti-HPV16 L1 by using AFM contact mode. For example, Fig. 2A and B show the typical force-distance curves for non-specific unbinding event and specific unbinding event, respectively. According to the phenomenon displayed on the force-distance curve which the non-specific unbinding event or specific unbinding event produces, we can acquire the results to analyze whether or not the sample includes HPV16.

In summary, we can identify much more effectively by AFM whether the subject is HPV16 patient from the proposed identification method and experimental results (as shown in Figs. 2, 3, and 4) in this paper.

Appendix A. Transparency document

Transparency document associated with this article can be found in the online version at http://dx.doi.org/10.1016/j.bbrep.2016.04.008.

References

[1] I. Cornet, T. Gheit, M. Iannacone, J. Vignat, B. Sylla, A. Del Mistro, S. Franceschi, M. Tommasino, G. Clifford, HPV16 genetic variation and the development of cervical cancer worldwide, Br. J. Cancer 108 (2013) 240–244.
[2] J. Koshiol, L. Lindsay, J.M. Pimenta, C. Poole, D. Jenkins, J.S. Smith, Persistent human papillomavirus infection and cervical neoplasia: a systematic review and meta-analysis, Am. J. Epidemiol. 168 (2008) 123–137.
[3] A. Karube, M. Sasaki, H. Tanaka, O. Nakagome, R. Dahiya, S. Fujimoto, T. Tanaka, Human papilloma virus type 16 infection and the early onset of cervical cancer, Biochem. Biophys. Res. Commun. 323 (2004) 621–624.
[4] A.P. Damin, R. Karam, C.G. Zettler, M. Caleffi, C.O. Alexandre, Evidence for an association of human papillomavirus and breast carcinomas, Breast Cancer Res. Treat. 84 (2004) 131–137.
[5] A. Di Lonardo, A. Venuti, M.L. Marcante, Human papillomavirus in breast cancer, Breast Cancer Res. Treat. 21 (1992) 95–100.
[6] N. Akil, A. Yasmeen, A. Kassab, L. Ghabreau, A. Darnel, A. Al Moustafa, High-risk human papillomavirus infections in breast cancer in Syrian women and their association with Id-1 expression: a tissue microarray study, Br. J. Cancer 99 (2008) 404–407.
[7] Y. Hasegawa, M. Ando, A. Kubo, S.-i. Isa, S. Yamamoto, K. Tsujino, T. Kurata, S.-H.I. Ou, M. Takada, T. Kawaguchi, Human papilloma virus in non-small cell lung cancer in never smokers: a systematic review of the literature, Lung Cancer 83 (2014) 8–13.
[8] C.B. Woodman, S.I. Collins, L.S. Young, The natural history of cervical HPV infection: unresolved issues, Nat. Rev. Cancer 7 (2007) 11–22.
[9] M. Schiffman, H. Bauer, A. Lorincz, M. Manos, J. Byrne, A. Glass, D. Cadell, P. Howley, Comparison of Southern blot hybridization and polymerase chain reaction methods for the detection of human papillomavirus DNA, J. Clin. Microbiol. 29 (1991) 573–577.
[10] C. Clavel, M. Masure, I. Putaud, K. Thomas, J.-P. Bory, R. Gabriel, C. Quereux, P. Birembaut, Hybrid capture II, a new sensitive test for human papillomavirus detection. Comparison with hybrid capture I and PCR results in cervical lesions, J. Clin. Pathol. 51 (1998) 737–740.
[11] G. Binnig, C.F. Quate, C. Gerber, Atomic force microscope, Phys. Rev. Lett. 56 (1986) 930–933.
[12] S. Ryu, Y. Hashizume, M. Mishima, R. Kawamura, M. Tamura, H. Matsui,

M. Matsusaki, M. Akashi, C. Nakamura, Measurement of cell adhesion force by vertical forcible detachment using an arrowhead nanoneedle and atomic force microscopy, Biochem. Biophys. Res. Commun. 451 (2014) 107–111.
[13] S.R. Nettikadan, J.C. Johnson, C. Mosher, E. Henderson, Virus particle detection by solid phase immunocapture and atomic force microscopy, Biochem. Biophys. Res. Commun. 311 (2003) 540–545.
[14] J. Sitko, E. Mateescu, H. Hansma, Sequence-dependent DNA condensation and the electrostatic zipper, Biophys. J. 84 (2003) 419–431.
[15] F. Valle, G. Dietler, P. Londei, Single-molecule imaging by atomic force microscopy of the native chaperonin complex of the thermophilic archaeon Sulfolobus solfataricus, Biochem. Biophys. Res. Commun. 288 (2001) 258–262.
[16] Y.G. Kuznetsov, S. Daijogo, J. Zhou, B.L. Semler, A. McPherson, Atomic force microscopy analysis of icosahedral virus RNA, J. Mol. Biol. 347 (2005) 41–52.
[17] P.Y. Meadows, J.E. Bemis, G.C. Walker, Single-molecule force spectroscopy of isolated and aggregated fibronectin proteins on negatively charged surfaces in aqueous liquids, Langmuir 19 (2003) 9566–9572.
[18] J. Kaur, K.V. Singh, A.H. Schmid, G.C. Varshney, C.R. Suri, M. Raje, Atomic force spectroscopy-based study of antibody pesticide interactions for characterization of immunosensor surface, Biosens. Bioelectron. 20 (2004) 284–293.
[19] Y. Chen, G. Zeng, S.S. Chen, Q. Feng, Z.W. Chen, AFM force measurements of the gp120–sCD4 and gp120 or CD4 antigen–antibody interactions, Biochem. Biophys. Res. Commun. 407 (2011) 301–306.
[20] J.W. Weisel, H. Shuman, R.I. Litvinov, Protein–protein unbinding induced by force: single-molecule studies, Curr. Opin. Struct. Biol. 13 (2003) 227–235.
[21] S. Allen, X. Chen, J. Davies, M.C. Davies, A.C. Dawkes, J.C. Edwards, C.J. Roberts, J. Sefton, S.J. Tendler, P.M. Williams, Detection of antigen-antibody binding events with the atomic force microscope, Biochemistry 36 (1997) 7457–7463.
[22] X.-E. Cai, J. Yang, The binding potential between the cholera toxin B-oligomer and its receptor, Biochemistry 42 (2003) 4028–4034.
[23] E. Kokkoli, S.E. Ochsenhirt, M. Tirrell, Collective and single-molecule interactions of $\alpha 5\beta 1$ integrins, Langmuir 20 (2004) 2397–2404.
[24] F. Kienberger, G. Kada, H. Mueller, P. Hinterdorfer, Single molecule studies of antibody–antigen interaction strength versus intra-molecular antigen stability, J. Mol. Biol. 347 (2005) 597–606.
[25] I. Lee, R.E. Marchant, Molecular interaction studies of hemostasis: fibrinogen ligand–human platelet receptor interactions, Ultramicroscopy 97 (2003) 341–352.
[26] G. Schochetman, C.-Y. Ou, W.K. Jones, Polymerase chain reaction, J. Infect. Dis. (1988) 1154–1157.
[27] B.T. Kurien, R.H. Scofield, Western blotting, Methods 38 (2006) 283–293.
[28] C. Stroh, H. Wang, R. Bash, B. Ashcroft, J. Nelson, H. Gruber, D. Lohr, S. M. Lindsay, P. Hinterdorfer, Single-molecule recognition imaging-microscopy, Proc. Nat. Acad. Sci. USA 101 (2004) 12503–12507.
[29] M. Yutsudo, T. Tanigaki, T. Tsumori, S. Watanabe, A. Hakura, New human papilloma virus isolated from epidermodysplasia verruciformis lesions, Cancer Res. 42 (1982) 2440–2443.